International Institute for Applied Systems Analysis
IIASA www.iiasa.ac.at

Address: IIASA, Schlossplatz 1, A-2361 Laxenburg, Austria
Email: permissions@iiasa.ac.at

Working paper

A neural network architecture for disaggregating age-specific population projections to the sub-national level

Andrea Tamburini, tamburini@iiasa.ac.at
Claudio Bosco, claudio.bosco@ec.europa.eu
Erich Striessnig, erich.striessnig@univie.ac.at

WP-03-2025

Approved by:

Name: Anne Goujon
Program: Population and Just Societies (POPJUS)
Date: 23 September 2025

Table of contents

ZVR 524808900

The authors gratefully acknowledge funding from the European Union under grant agreement No 101081369 (SPARCCLE).

Abstract

Improving our understanding of future risk from climate change requires realistic projections of future populations, both in their size and distribution. Distribution refers not only to geographic breakdowns but also to the breakdown by important characteristics, such as age. While the location where people will live may determine future exposure to hazards, population characteristics also co-determine the degree of vulnerability and the capacity to adapt to changing environmental conditions. Despite the importance of these factors, there remains a paucity of population projections (or disaggregations thereof) at the sub-national level. We develop a machine learning-based model to disaggregate age-specific population projections based on the Shared Socioeconomic Pathways (SSPs) to the sub-national NUTS-2 level for 34 European countries. Our focus on Europe is driven by its high degree of spatial variability, both in terms of climatic conditions and population structure, as well as the rapid pace of climate change and population aging there.

About the authors

Andrea Tamburini is a researcher at the Population and Just Societies (POPJUS) Program in IIASA and PhD candidate at the Department of Demography at the University of Vienna (Contact: tamburini@iiasa.ac.at).

Dr. Claudio Bosco is project officer in Demography and Migration (JRC.E.5) group at the Joint Research Center of the European Commission (Contact: claudio.bosco@ec.europa.eu).

Assoz. Prof. Erich Striessnig is Associate Professor at the University of Vienna and the Deputy Head of the Department of Demography. He is also a Senior Researcher at IIASA's Population and Just Societies (POPJUS) Program (Contact: erich.striessnig@univie.ac.at).

Acknowledgments

The authors gratefully acknowledge funding from the European Union under grant agreement No 101081369 (SPARCCLE).

1 Introduction

The assessment of climate-related mortality and morbidity risks requires a systematic understanding of demographic developments. The composition of the population and its geographical distribution are essential to infer about the future impact of extreme climatic events and to estimate the adaptation and mitigation capacities of a region's inhabitants. The impact of climate change is not distributed evenly across geographical regions and population subgroups. Even within the same country, physical and socioeconomic characteristics of a region and its population can influence the extent of exposure and the degree of vulnerability.

In terms of demographic characteristics, age is probably the most critical factor in climate-related mortality. Newborns, children and the youth suffer disproportionately from the effect of anthropogenic climate change, from the direct effect on increased neonatal and child mortality to systematically increased stress levels.

Newborns, children, and adolescents are disproportionately affected by anthropogenic climate change (Weeda et al. 2024), ranging from elevated risks of neonatal and child mortality (Dimitrova 2021; Thiede and Gray 2024) to systematically increased stress levels (McMichael 2014). Furthermore, climatic shocks such as floods and droughts have been shown to heighten mortality risk in these groups, both directly and indirectly, through their impacts on food security and malnutrition (Basu 2009; Freudenreich et al. 2022; Dimitrova 2021). At the other extreme of the age distribution, numerous studies have consistently identified the elderly as a particularly vulnerable group (for a recent survey see Son et al. 2019). Older adults face a higher risk of mortality from both heat and cold exposure, potentially due to physiological changes, different activity patterns, housing quality, and social factors. The physiological factors may include limited thermoregulatory response capabilities, a higher prevalence of pre-existing comorbidities, and reduced access to social services, which can exacerbate the impact of extreme temperatures (Rai et al. 2022).

Going forward, recent projections suggest that the number of deaths will be highest among those aged 85 years and older, an age group that is both more susceptible to extreme temperatures and expected to grow substantially in the future (García-León et al. 2024). When considering the overall effect of both cold- and heat-related mortality, the balance is expected to remain highly positive for this age group, particularly in warmer climate scenarios, with regional disparities in present risks and increases with warming, especially for heat-related mortality (Lloyd et al. 2023). The contribution of demographic forces to increased future temperature-related mortality is largely driven by population ageing, especially for cold-related mortality due to higher relative risks among the elderly. Hotspots of heat-related mortality are often determined by the combination of increased susceptibility associated with ageing and increased hazard due to warming temperatures.

The combination of the spatial distribution of aging and future climate impacts is, therefore, important for tracking vulnerability (McDermott-Levy et al. 2021; Calleja-Agius et al. 2021).

Despite the obvious importance of understanding, not only where people live but also who they are, there remains a paucity of projections (or disaggregation thereof) at the sub-national geographical level that also include demographic heterogeneity, e.g., age structure.

In their most up-to-date population projections, KC et al. (2024) provide age, sex, and education-specific population projections in five-year steps until 2100 for 201 countries consistent with the Shared Socioeconomic Pathways (SSPs). The SSPs are a set of global scenarios describing alternative trajectories of societal development, designed to facilitate the integrated analysis of future climate impacts, vulnerabilities, and adaptation or mitigation challenges. They combine assumptions about demographic change, economic growth, technological development, and other socioeconomic drivers to produce internally consistent narratives and quantitative projections. However, results of these multidimensional population projections are only available at the country level. For climate risk assessments, this resolution is too coarse to support the identification of vulnerable sub-groups according to regional climatic conditions. Much of the impact of climate change on human populations will be locally confined, so a further geographical breakdown is urgently needed in the context of environmental and climatic research. This geographical disaggregation of population projections and urban land projections has been provided at high spatial resolution by Gao (2020) and Gao and Pesaresi (2021), respectively. While these projections shed light on current and future population distribution at a highly refined geographical scale (1 square km), they contain no information about population composition. Wang, Meng, and Long (2022) introduced an alternative approach for global-scale projections, while other works have focused on the country-level (Yimin Chen et al. 2020; Xu et al. 2024) or specific urban areas (Kang and Lee 2024).

Considerable advancements have been made in recent years regarding attempts to disaggregate the SSPs to the subnational level while preserving their multidimensionality. For instance, Yidan Chen et al. (2020) developed a dataset of China's population from 2010 to 2100 at the provincial level, disaggregated by age, sex, and seven educational levels under the five SSPs. This study employed a recursive multidimensional model that integrates fertility, mortality, migration, and educational progression rates, while also accounting for China's fertility policies and population ceilings in megacities. Furthermore, the model projected urbanization rates based on historical trends. Similarly, Hauer (2019) provided highly detailed projections (by age, sex, and race) at the county level for the United States. These projections were generated using cohort-change ratios (CCRs) and cohort-change differences (CCDs) projected through an ARIMA model. In this paper, the SSPs play a crucial role in controlling the population projections, but they are not directly disaggregated to the county level. Instead, the study uses SSPs as aggregate constraints to ensure the projections align with broader socioeconomic scenarios and to prevent unrealistic population growth or decline.

In contrast, Striessnig et al. (2019) utilized regression trees trained on historical census data (1980–2010) to directly downscale national-level SSP projections to the county level. This method accounted for spatial variations and historical demographic trends, projecting five broad age groups (0–19, 20–29, 30–54, 55–69,

70+). Additional subnational projections are available from national statistics offices, such as those in the United Kingdom[1] and New Zealand[2].

A common pattern observed in all these studies is the trade-off between incorporating detailed population characteristics, such as age structure, and maintaining a multi-country scope in the studies and methods developed. Methods that disaggregate multi-national projections (e.g., SSPs) primarily focus on global narratives, often at the expense of detailed population characteristics. In contrast, single-country or urban-region studies tend to preserve these characteristics while sacrificing broader geographic coverage.

A subnational age structure projection is essential for assessing climate-related risks at a more granular level, as demographic trends, particularly ageing, play a crucial role in shaping vulnerability to climate impacts such as heat stress, air pollution, and respiratory illnesses. The European Climate Risk Assessment (European Environment Agency. 2024) highlights that Europe's ageing population is a growing concern, with heat-related mortality projected to increase tenfold under 1.5°C warming scenario and thirtyfold under 3°C. Additionally, an ageing population combined with existing health conditions is expected to heighten the burden of climate-related diseases, particularly in regions already experiencing demographic decline. Given that many climate risks, including ecosystem disruptions, food security challenges, and infrastructure vulnerabilities, extend beyond national borders, a detailed demographic perspective at the subnational level is crucial. It enables more precise climate risk assessments, informs adaptation strategies, and supports coordinated policy responses across Europe to address shared climate challenges effectively.

For the subnational disaggregation of age-specific populations in European countries, Terama et al. (2019) employed a scaling method. This approach downscaled national-level age structure projections, derived from a cohort-component model, to subnational regions based on their age structures in the base year. However, this method does not account for temporal changes in the relative age distribution across regions.

Eurostat, the statistical office of the European Commission, has developed a product linked to EUROPOP2019, the most recent set of population projections for 31 countries. These projections cover all 27 European Union (EU) Member States and four European Free Trade Association (EFTA) countries, spanning the period from 2019 to 2100. Rather than serving as forecasts, these projections represent 'what-if' scenarios, designed to illustrate potential future demographic trends based on specific assumptions. Subnational projections are provided at the NUTS-3 level for multi-regional countries, with the exception of Cyprus, Luxembourg, and Liechtenstein. The Nomenclature of Territorial Units for Statistics (NUTS) is a hierarchical system used to divide the economic territory of the EU and the UK, facilitating the collection, harmonization, and analysis of regional statistics, socioeconomic research, and the development of EU regional policies.

---

1 https://www.ons.gov.uk/peoplepopulationandcommunity/populationandmigration/populationprojections/bulletins/subnationalpopulationprojectionsforengland/2018based

2 https://www.stats.govt.nz/information-releases/subnational-population-projections-2018base2048/

This work resulted in a dataset containing yearly projections for single-year age groups for both females and males, with unprecedented geographical detail. These projections are based on purely demographic scenarios rather than the standardized narratives typically used in climate change research.

The Shared Socioeconomic Pathways (SSPs) offer significant advantages for climate change research and policy planning. SSPs provide a coherent framework for exploring alternative futures with varying challenges for climate change mitigation and adaptation (Merkle et al. 2023). When combined with Representative Concentration Pathways (RCPs), they enable more comprehensive assessments of climate impacts, adaptation, and vulnerability (Van Ruijven et al. 2014). Building on this foundation, we directed our efforts toward creating a disaggregation approach tailored specifically for the climate change research community. The present study aims to develop a machine learning-based model to generate sub-national age-specific population projections for 34 European countries at the NUTS-2 level, extending to the year 2100. NUTS-2 regions represent the relevant geographical framework for implementing EU regional policies (Eurostat, 2024). This study area ensures a high degree of variability, both in terms of population structure (Kashnitsky and Schöley 2018) and climatic conditions (Büntgen et al. 2011; Jylhä et al. 2010).

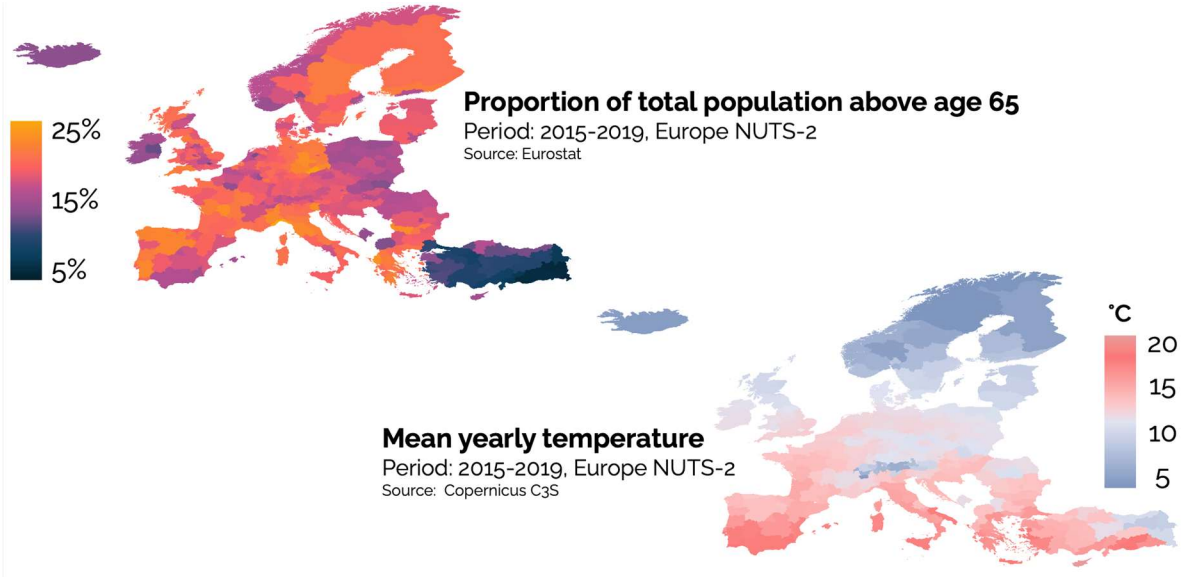

Figure 1: Distribution of the population aged over 65 years (left panel) and mean yearly temperature (right panel) at the NUTS-2 level.

Section 2 presents the data and modelling framework, including the scenario basis, empirical foundation, modelling strategy, spatial dimension, and model architecture. Section 3 reports the results, and Section 4 provides a discussion of the main findings together with directions for future development. References and supplementary material conclude the paper.

2 Data and model

2.1 SSPs

Providing details on the SSPs framework at the outset of this section is crucial, as the selection of data sources and the construction of variables in this study are inherently dependent on the specific SSP scenario considered. In what follows, we present the assumptions underlying the population projections for Europe, as this constitutes the geographical scope of our analysis.

• SSP1 (Sustainability/ Rapid Social Development): For low-fertility European countries, this scenario assumes low10 fertility, low mortality, and medium migration. This combination of very low birth rates and longer lifespans, even with some immigration, is likely to lead to significant population aging, although the migration might moderate the pace to some extent.
• SSP2 (Middle-of-the-Road/Continuation): For low-fertility European countries, SSP2 assumes medium fertility, medium mortality, and medium migration. While 'medium fertility' might still be below replacement level in many European contexts, it suggests a less rapid fertility decline than SSP1. Combined with medium mortality and migration, this scenario would likely still result in population aging, but perhaps at a more gradual pace compared to scenarios with lower fertility.
• SSP3 (Fragmentation/Stalled Development): Low-fertility European countries under SSP3 are projected to have low fertility, high mortality, and low migration. This combination of low birth rates, shorter lifespans, and limited immigration would likely lead to pronounced population decline and significant aging, as fewer young people are born and survive to older ages, and emigration is not sufficiently offset by immigration.
• SSP4 (Inequality): For low-fertility European countries, SSP4 assumes low low fertility, med mortality, and high migration. The extremely low birth rates would strongly drive rapid aging. While high migration could bring in younger individuals and potentially slow the aging process compared to scenarios with lower immigration, the fundamental imbalance of very few births against a backdrop of longer lifespans (implied by medium mortality) would likely still result in a significantly older population.
• SSP5 (Conventional Development): Low-fertility European countries in SSP5 are projected to have low10[3] fertility, low mortality, and medium migration. Similar to SSP1, the very low fertility rates, coupled with longer lifespans, would contribute significantly to population aging. Medium migration could offer some counteraction by adding younger cohorts, but the underlying driver of very low birth rates suggests that aging would still be a substantial trend.

In essence, all SSP scenarios indicate that Europe will experience population aging due to low or declining fertility and increasing life expectancy. The speed and degree of aging are most significantly influenced by the assumed levels of fertility and migration in each scenario. Scenarios with very low fertility and limited migration depict the fastest and most pronounced aging.

[3] The Low10 fertility scenario is an additional low-fertility scenario where education-specific Total Fertility Rates (TFRs) are 10% lower than the medium fertility assumptions up to the year 2040, with the difference subsequently increasing to 12.5% lower than the medium fertility assumptions by 2060 and remaining at that level until 2100. This scenario is specifically used in SSP1 and SSP5 for low-fertility countries.

2.2 Empirical Basis

Our sub-national disaggregation of the SSPs is based on three main data sources, providing population-related information for Europe:

1- The Eurostat Database[4]: provides the NUTS-2 breakdown of the age-specific baseline population across 34 countries. The information is reported yearly starting from 1990 until 2023 and for five-yearly age groups from "under 5" up to "75+".

2- The Wittgenstein Centre Data Explorer[5] (WCDE): provides SSPs-coherent, age-specific population information at the country level for 2020-2100. The projections are available for a total of 200 countries, of which 39 in Europe for five-yearly age groups from "under 5" up to "100+" (KC et al. 2024).

3- Harvard Dataverse[6]: provides the "Global 1-km Downscaled Urban Land Fraction Grids, SSP-Consistent Projections and Base Year, v1 (2000 - 2100)" (Gao and Pesaresi 2021) and the "Global 1-km Downscaled Population Grids, SSP-Consistent Projections and Base Year, v1.01 (2000 - 2100)" (Gao 2017; 2020). This downscaled information can be aggregated to the NUTS-2 level to generate total population counts and urban land fractions to be used in the construction of the independent variables.

Population totals derived from the three data sources do not necessarily match, as they are relying on different inputs. Even the two SSP-coherent sources of information differ due to (Gao 2017; 2020) being based on an earlier version of the human capital projections (Lutz et al. 2014). In light of this, we adjusted and standardized all data to align with Eurostat values, using the 2020–2024 Eurostat figures as the reference for correcting the other sources, thereby ensuring general coherence for both historical observations and future projections through a simple proportional approach.

2.3 Modelling approach

The SSPs-consistent age-disaggregation is inspired by Striessnig et al. 2019. The approach presented there involves developing a set of separate models, one for each selected age group, which predict the share of the total population belonging to the respective age group within each county of the US. This proved necessary due to the complexity of the overall task and the difference in drivers of population dynamics within different

[4] https://ec.europa.eu/eurostat/databrowser/explore/all/all_themes?lang=en&display=list&sort=category
[5] https://dataexplorer.wittgensteincentre.org/wcde-v3/
[6] https://dataverse.harvard.edu/

sub-populations. By breaking down the overall task into smaller, less complex assignments, the aggregate results became more accurate and also interpretable.

After conducting extensive exploratory data analysis, we categorized the European population at the NUTS-2 level into five age groups: under 15, 15–24, 25–44, 45–64, and 65 and above. This classification was designed to capture differences in climate change vulnerability and adaptation needs across various societal segments while also accounting for the spatial distribution of each group. The distinction between those under 15 and those under 25 acknowledges the special characteristics of large university centers, which tend to have higher shares of young adult populations and lower labor force participation of the population under the age of 25. The 25–44 age group represents younger adults, often in the early stages of family formation, whereas the 45–64 age group encompasses individuals at later career stages, leading up to retirement. Finally, the open-ended 65+ category represents the population beyond the conventional working age. Based on this categorization, we develop a disaggregation model tailored to each age group.

The difficulties related to limited data availability and the need to integrate national-level scenarios, as noted by Striessnig et al. (2019) were further amplified in a multinational framework. Since demographic processes such as changes in population structure unfolded slowly but had lasting consequences, it was essential to apply a modelling strategy that ensured the highest possible predictive accuracy. Artificial neural networks (ANNs) provided a clear advantage over regression trees in this regard, as they captured complex non-linear relationships, interpolated and extrapolated beyond observed data, modelled smooth continuous trends, and generalized effectively (Zou et al. 2008). These features made ANNs particularly well suited to identifying the subtle patterns and dynamics that characterized demographic evolution. In our modelling framework, we therefore employed a machine-learning architecture based on ANNs, which also allowed for uncertainty quantification regarding the predictions. ANNs are computational models inspired by the functioning of the human brain, consisting of interconnected layers of artificial neurons—basic computational units that receive input signals, apply weighted transformations, and pass the output to subsequent neurons. These connections between neurons are governed by learnable weights that determine the strength of the influence one neuron has on another. Each neuron typically applies an activation function to introduce non-linearity, enabling the network to learn complex relationships within the data. Among the various types of ANNs, feedforward neural networks (FNNs) are the simplest and most widely used architecture (Carvalho et al. 2011; Schmidhuber 2015). In an FNN, information flows in a single direction—from input nodes through hidden layers to output nodes—without looping back. The universal approximation theorem, introduced by Hornik, Stinchcombe, and White (1990), demonstrated that FNNs with at least one hidden layer and a non-linear activation function can approximate any continuous function, given sufficient neurons and proper training. This theorem underscores the immense modelling potential of neural networks across a wide range of applications (White 1989). Moreover, Rumelhart, Hinton, and Williams (1986) introduced the backpropagation algorithm, a powerful technique for efficiently computing the gradients needed to update the weights of network layers, which can be efficiently used in combination with gradient descent. This breakthrough fundamentally transformed neural network training and facilitated their widespread adoption in research and industry.

ANNs are sensitive to initial weight selection, particularly with small training sets (Nguyen and Widrow 1990)(add citation). The pattern error surface of ANNs contains numerous local minima, which are deeper and more abundant when training samples are limited (Raudys and Skurikhina 1992). This sensitivity can impact network performance, as the initial weights influence the training process and final outcome. To

address this issue, researchers have proposed various strategies, including adding noise to training vectors (Raudys and Skurikhina 1992) using particle swarm optimization for pre-training (Nikelshpur and Tappert 2013), and employing sensitivity analysis for selective learning (Engelbrecht 2001). Moreover, successful training via Stochastic Gradient Descent (SGD) tends to leave the network weights in close proximity to their initial configuration (Jesus et al. 2021). These findings highlight the importance of careful weight initialization, especially when working with small training sets. To address this point, enhance model performance and incorporate a measure of uncertainty while maximizing the use of our limited training data, we employed a simplified version of the Selective Improvement Evolutionary Variance Extinction (SIEVE) framework (De Rigo et al. 2005) as detailed in Bosco et al. (2018). This approach was applied to our FNNs.

Simplified SIEVE

This framework aims to efficiently select the most promising set of initial weights in a FNN by dynamically allocating computational resources during training. Instead of uniformly distributing the training effort across all randomly initialized weight sets, the approach progressively focuses on those that demonstrate superior performance in terms of mean absolute error (MAE), dedicating an increasing number of epochs—where one epoch corresponds to a complete pass through the entire training dataset—to their optimization. The MAE was chosen over RMSE because it is less sensitive to large outliers, providing a robust measure of average prediction error in the original units of the dependent variable (Willmott and Matsuura 2005).

To apply the simplified SIEVE approach to our problem of finding the optimal sub-national distribution by age of available national-level projections, we estimated a collection of models for each selected age group ("under 15," "15–24," "25–44," "45–64," and "65+"). Following an initial correlation analysis and hyperparameter optimization, we adopted a three-round (selections) simplified SIEVE approach with an initial training phase of 5 epochs:

1. Initialization: We generated 625 different sets of initial weights and trained each model for 5 epochs.
2. First selection: The top 125 models (25 per age group), based on performance, were selected and further trained for 25 epochs.
3. Second selection: From these, the 25 best-performing models were chosen and trained for 125 epochs.
4. Third selection: The 5 highest-performing models were retained.

The procedure, summarized in the following pseudo-code, is repeated 20 times. In each iteration, the performance of the models is evaluated via MAE on both training and validation sets, and the top 100 best-performing models for each age group are selected. This results in a collection of 100 models per age group after completing all iterations.

```
Step 0: Initialize and train first set of models
models = initialize_models(625)  # 625 different initial weight sets
train(models, epochs=5)
performance = evaluate(models)

Step 1: Select top 125 models and continue training
top_125 = select_top_models(models, performance, top_k=125)
train(top_125, epochs=25)
performance = evaluate(top_125)
```

```
Step 2: Select top 25 models and continue training
top_25 = select_top_models(top_125, performance, top_k=25)
train(top_25, epochs=125)
performance = evaluate(top_25)

Step 3: Select the top 5 models
top_5 = select_top_models(top_25, performance, top_k=5)
```

2.4 The Spatial Dimension

Several attempts were made to enrich the disaggregation model with a spatial dimension. While the case addressed in Striessnig et al. 2019 requires only the modelling of spatial differences within one country (the United States), we are faced with the challenges of modelling multi-country data from European NUTS regions. Besides influencing the choice of the dependent variable, this also adds a challenge in terms of the learning potential of the model. Given the diverse context of Europe, we are faced with issues related to heterogeneous data availability and the necessity to efficiently make use of what harmonized information is available. As an initial step, we computed Moran's I for the spatial distribution of population in 5-year age groups at different time points in the past. This initial analysis did result in moderate levels of positive spatial autocorrelation[7], which never exceeded 0.2. This is likely due to two main reasons:

1. **Border regions**: NUTS-2 regions that share at least one border with a NUTS-2 region from a different country represent a challenge to spatial analysis. Due to the diverse population structures of neighbouring countries, a simple queen-style approach to defining neighbourhood, or any other approach that does not account for country-specific characteristics, is inadequate for our needs. Therefore, alternative methods need to be explored to account for the complex spatial relationships between regions. As an example, Figure 2 depicts the marked discontinuity in terms of the proportion of population aged 65+ between Germany and some of its neighbouring countries, particularly in the East of Europe.

[7] Considering the polygonal geometry of the spatial entities we opted for a Queen neighbourhood definition

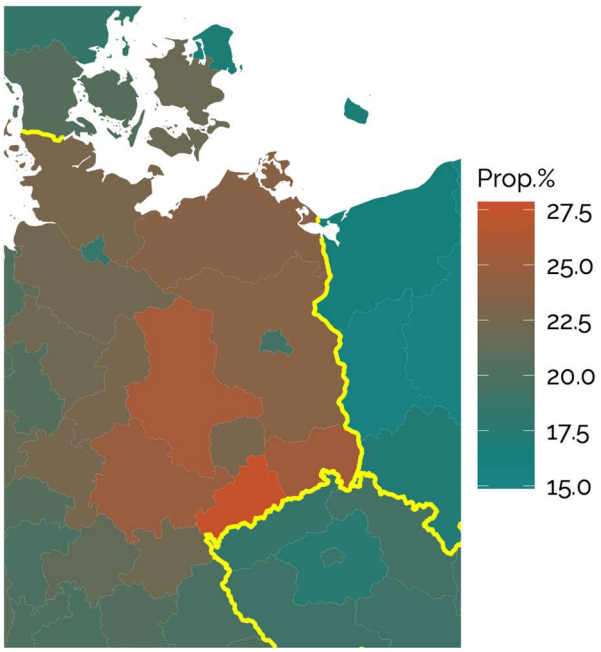

Figure 2: An example of bordering regions. Here we show the proportion of the total population in the age group '65+' in the interval 2015-2019 focusing on the regions in eastern Germany, Poland and Czechia.

2. Large agglomerations: these are regions that exhibit a distinctive structure in comparison to others, typically due to their high degree of urbanization, which is often associated with being a main or capital city (and the immediately surrounding area). As shown in Figure 3, Hamburg and Berlin in Germany are two such "outlier" regions characterized by population structures, which are a result of their unique economic and political conditions.

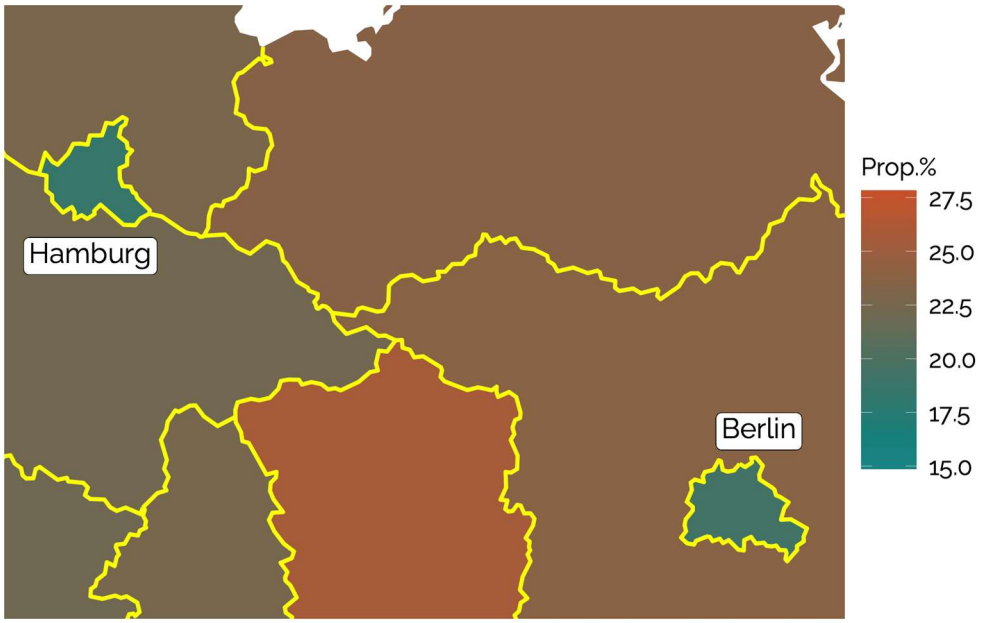

Figure 3: An example of "urban islands". Here we show the proportion of the total population in the age group '65+' in the interval 2015-2019 focusing on the NUTS-2 regions of Berlin and Hamburg compared to the ones surrounding them.

To tackle the problems posed by different countries in our sub-national analysis, we take advantage of the communal structure observed among trans-border clusters of regions. We assume that regions belonging to different countries might be more similar in terms of population structure than non-adjacent regions in the same country. As an initial attempt, we defined hierarchical clusters of NUTS-2 regions based on a 5-dimensional vector representing the population structure, with respect to the national one, over the 2015-2019 period. To ensure equal contribution from each dimension of the vector, we first normalized the data, addressing the potential for disproportionate influence among the age group proportions. Following this, we apply Principal Component Analysis (PCA) to reduce the number of dimensions while retaining the primary sources of variation in the dataset. By selecting the first three principal components, we also minimize the noise, simplifying the clustering process using Ward's method (Ward 1963). After examining the resulting dendrogram, we chose to cut the tree at three clusters, as this provides a balance between cluster size and interpretability. Ultimately, the clustering procedure was applied to 306 regions, which were grouped into three clusters of sizes 154, 96, and 56, respectively. The combination of normalization, PCA, and hierarchical clustering allows us to uncover natural groupings of regions based on the evolution of their population structure, providing valuable insights into the spatial patterns of demographic changes across countries. Figures 4 represents the results of the clustering exercise geographically. Clearly, clusters are not just delineated by national borders.

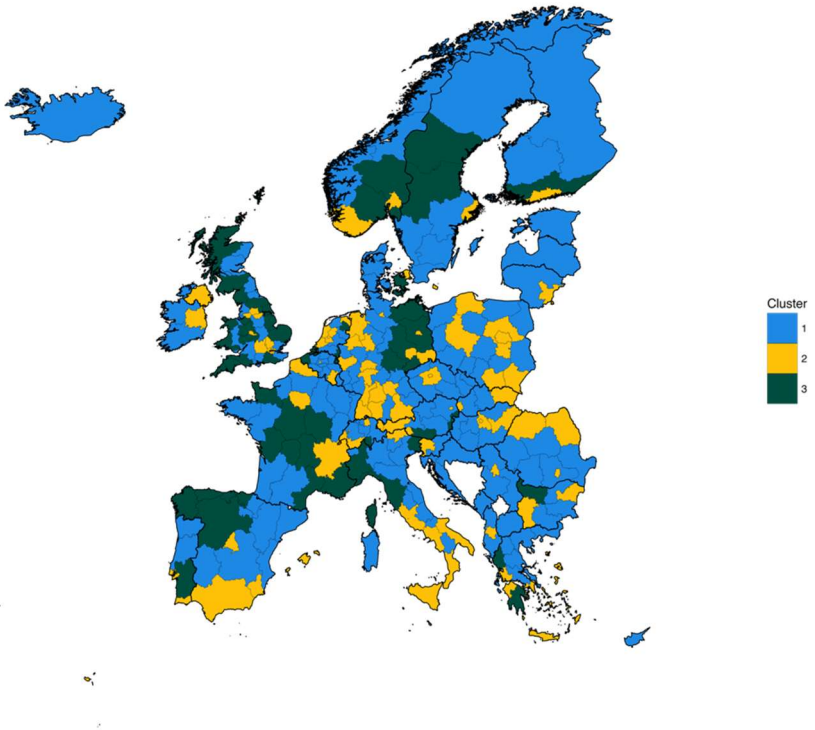

Figure 4: Clusters of regions based on the evolution of age structure. The map displays the three clusters identified using a hierarchical clustering procedure, with colors indicating cluster membership.

Figure 5 presents the evolution of the ratios between the regional- and the national-level age-group proportion (linearly approximated across all regions within each cluster). Cluster 1, the largest, includes regions where the age structure closely aligns with the national-level pattern. Cluster 2 primarily consists of regions encompassing capital cities or major economic centers, which exhibit a significantly higher share of younger population—particularly in the first three age groups—indicating potentially higher fertility rates. In contrast, Cluster 3 comprises regions characterized by an older demographic structure, with the population aged 45 and above consistently exceeding the national-level proportion.

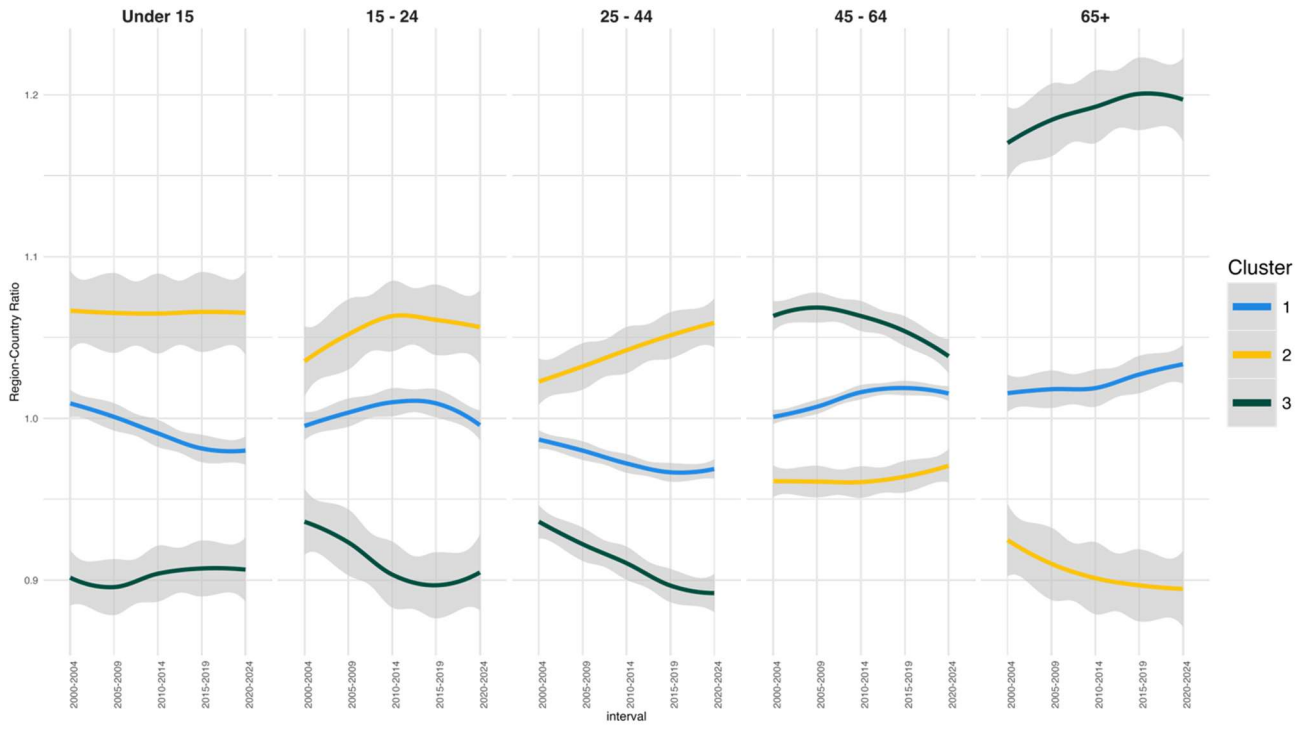

Figure 5: Region to country proportions by age group and cluster, European NUTS-2 region, 2000-2024.

2.5 Model architecture, fitting and performance

Given that our study focuses on the disaggregation of existing totals from previous projection efforts, rather than on absolute values, we emphasize proportions of population within different age-groups. Consequently, our quantities of interest—our dependent variables—are defined as the ratios between the population share of a specific age group at the subnational level and the corresponding national-level share (within the same country). These ratios are straightforward to interpret: values above 1 indicate a higher proportion of the population in a given age group compared to the national average, whereas values below 1 indicate a lower proportion. Furthermore, these ratios can be easily converted into absolute population figures using the existing, sub-national totals derived from the original SSPs (Gao 2020). In sum, this approach enables us to combine the existing, high-resolution total population projections at the subnational level and the multi-dimensional one at the national level. Moreover, this formulation makes the inclusion of the different scenario pathways straightforward.

We denote the proportion of the population of age-group a at time t in the NUTS-2 region i as $Prop^t_{a,i}$. The same portion at the national level is denoted as $Prop^t_{a,ctry}$. Thus, the dependent variable is defined as

$$y^t_{a,i} = \frac{Prop^t_{a,i}}{Prop^t_{a,ctry}}$$

As the set of age-groups is fixed, we drop the corresponding subscript from the notation for readability.

For each age group, the set of covariates includes the complete historical evolution of the region's age structure over the preceding 10 years. This is achieved with 5 and 10 years lagged variables, capturing changes in age group proportions over time. Additionally, it incorporates regional-level characteristics such as the degree of urbanization, the total population and its growth/decline, national-level age-structure information (e.g.: age group proportions at the national level), and the region's cluster assignment. This results in a total of 53 covariates which are listed in Table A1. For each age-group, we obtain a data set in tabular format of 1245 observations.

The large number of explanatory variables, coupled with a limited number of training points, required the careful application of a thorough preprocessing strategy. This aimed to improve training efficiency by reducing redundancy while enhancing model interpretability—addressing the common perception of neural networks as black-box models. The simplified-SIEVE procedure played a crucial role in optimizing the use of limited training data. Preprocessing involved removing redundant columns and calculating pairwise correlations to filter highly correlated predictors, initially using a Pearson correlation threshold of 0.9. To capture more general dependencies, a distance correlation matrix (Székely et al. 2007) was computed, flagging variables exceeding a threshold of 0.65 for further investigation. Unlike Pearson correlation, which primarily detects linear relationships and can be zero even when variables are indeed strongly connected in other ways, distance correlation is zero if and only if the variables are truly independent, making it a more comprehensive measure of dependence.

To ensure a balanced representation of all clusters and time periods in each age-specific subset, the dataset was stratified—i.e., partitioned, such that the distribution of these factors was preserved across splits. Using random subsampling, the data were then divided into training, validation, and test sets in proportions of 70%, 15%, and 15%, respectively. Standardization, which scales input features to have zero mean and unit variance, was applied to prevent data leakage, ensuring consistency across all splits. Hyperparameter tuning was performed via grid search to optimize the number of hidden units, defined as the neurons in the network's hidden layers, learning rate, and activation function. To refine variable selection, a Jackknife-style procedure iteratively excluded one of each pair of highly correlated variables, retaining the one contributing more to explained variance. The final model was then trained with the selected covariates according to the simplified-SIEVE procedure and evaluated on the test set using the median of the forecasted values as estimates. This approach ensured robust performance while minimizing overfitting and maintaining the representativeness, consistency, and reliability of the dataset during the modelling process.

Model performance was assessed using both the explained variance (Exp.Var.), and the RMSE and its performance was compared to the one of two simple models. A trivial model, which repeats the last available ratio observation as forecast ("*repeater*") and a slightly more sophisticated one, which returns the mean of the previously observed ratios as forecast ("*meaner*"). Table 1 reports the *Exp.Var.* and *RMSE* values for the model that was selected (Simp-SIEVE-NN) compared to the simple models for the 5 different age groups for the rescaled values, i.e., the population proportions at the sub-national level, which are our final quantities of interest, and not the ratios directly obtained from the modelling exercise.

Age group	Model	Test-Exp.Var.	Test-RMSE
Under 15	***Simp-SIEVE-NN***	**0.937**	**0.020**
	repeater	0.814	0.0345
	meaner	0.753	0.045
15 - 24	***Simp-SIEVE-NN***	**0.857**	**0.030**
	repeater	0.803	0.035
	meaner	0.430	0.062
25 - 44	***Simp-SIEVE-NN***	**0.967**	**0.012**
	repeater	0.942	0.016
	meaner	0.795	0.029
45 - 64	***Simp-SIEVE-NN***	**0.932**	**0.012**
	repeater	0.862	0.016
	meaner	0.616	0.030
65+	***Simp-SIEVE-NN***	**0.974**	**0.018**
	repeater	0.943	0.026
	meaner	0.887	0.044

Table 1: model performance in the test set with comparisons.

The Simp-SIEVE-NN technique demonstrates a high level of explained variance across all age groups, consistently exceeding 0.9, except for the 15–24 age group, where Exp.Var. remains strong at 0.857. This lower performance is likely due to the high spatial mobility within this age group, which includes both high school students and highly mobile students in higher education. Notably, even trivial models struggle with this age group. Despite this challenge, the model outperforms both trivial models, although the repeater model maintains a relatively strong performance. This is an important aspect to consider, as the model is designed to forecast population structure changes over five-year intervals. Given the slow and, in some cases, stable nature of demographic shifts in Europe, simply repeating the last observed value can yield reasonably accurate predictions.

However, the precision of our model reassures us of its ability to interpret and capture the interplay between covariates and detect subtle variations. Such sensitivity is crucial in demographic processes, where small shifts can lead to significant long-term effects. Moreover, this capability makes the model well-suited for integrating scenario narratives, allowing it to reflect potential shifts in population structure due to external influences.

Another key feature of our projection model is its uncertainty quantification, which is inherited from the Simplified SIEVE approach. Instead of producing a single predictive model, this method generates a family of models (in our case, 100), allowing us to assess the stability of different neural networks in forecasting the proportion ratios.

Figure 6 presents faceted caterpillar plots of our predictions, where the line extremes represent the 0.025 and 0.975 quantiles for each predicted value across different test sets and age groups. The green dots indicate the median predictions, while the true values are marked with red crosses. This visualization not only highlights the model's ability to closely estimate test set ratios, but also demonstrates that, in nearly all cases, the true values fall within the predicted quantile intervals, confirming the model's robustness in capturing age structure variations.

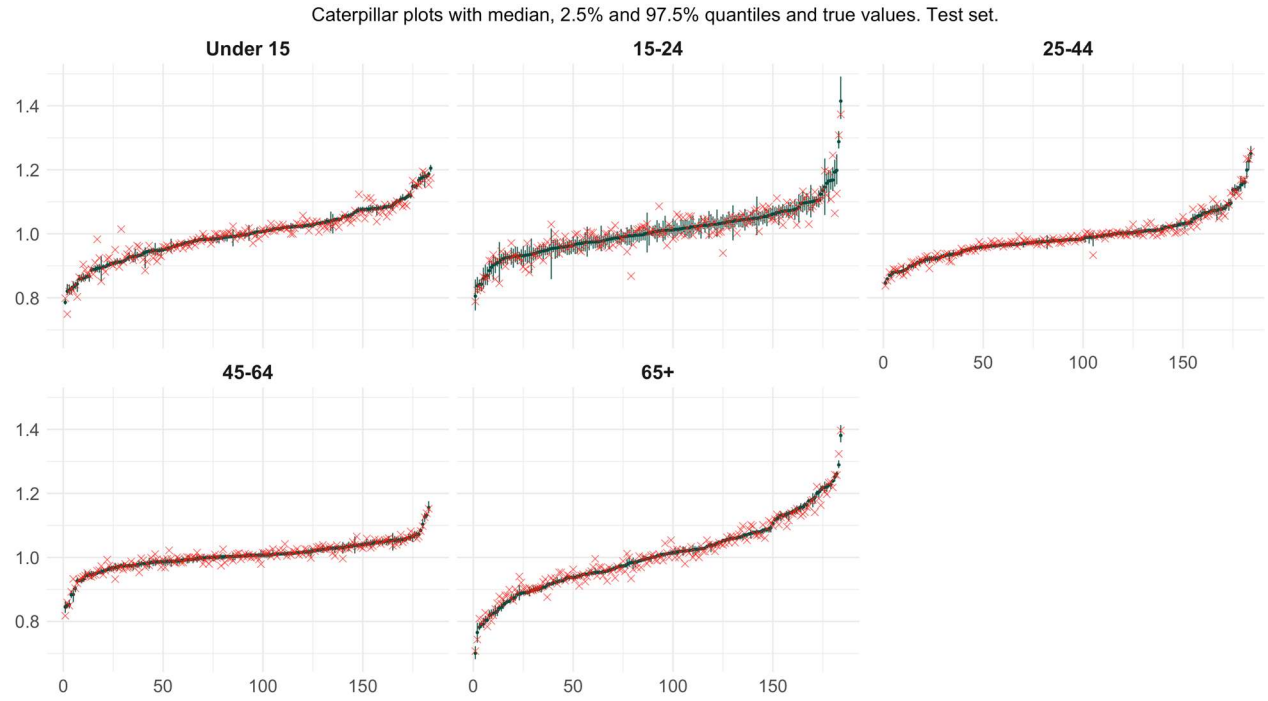

Figure 6: Caterpillar plots. The figure shows the 100 predictions from the SIEVE-NN models (median, 2.5% quantile, and 97.5% quantile in green), ordered by magnitude for readability. True values for the test set are indicated by red crosses.

3 Results

Our sub-national projections are developed as a disaggregation of the Wittgenstein Centre's global population and human capital projections at the national level. These projections based on the Shared Socioeconomic Pathways (SSPs), are primarily shaped by assumptions regarding fertility and migration, highlighting the significant role of demographic dynamics in future population structures.

Having this as starting point, we used the national level population structure, the NUTS-2 SSP-specific projections for the total population and the urbanization percentage, obtained aggregating the 1-km2 SSP-consistent downscaled projection grids, and applied the 5 age-group-specific estimated models to recursively produce a set of subnational (NUTS-2) disaggregation of the national level results.

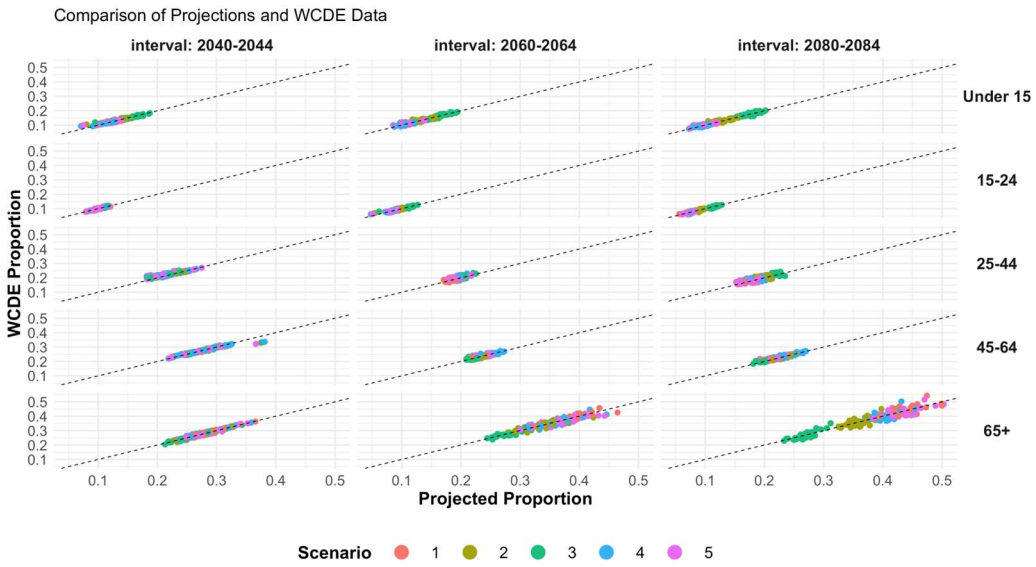

Figure 7: scatter plot of existing WCDE projections and our results when grouped according to the age group.

We validate our projection results in several steps. First, we compared regional-level outcomes according to their respective countries to the existing results from the national-level, cohort-component-based projections. As shown in Figure 7, the results are reassuring: a strong alignment with the diagonal indicates high accuracy. The age group '65+' exhibits the greatest variations, particularly under SSP 5. This is likely due to its open-ended nature, which encompasses a broader population range, as well as the pronounced aging patterns that our model captures in certain regions. Importantly, we deliberately chose not to apply a constraining step—such as Iterative Proportional Fitting (IPF)—that could have ensured even greater adherence to national-level results. Instead, we prioritized the development of subnational patterns over absolute coherence with national-level projections. While absolute coherence was ensured by construction in terms of total population at the regional level, we did not impose the constraint that age-specific regional populations must sum exactly to the corresponding national totals. This choice allowed the model greater flexibility to capture subnational trends, enabling age structures to be modelled more directly and with fewer externally imposed boundaries.

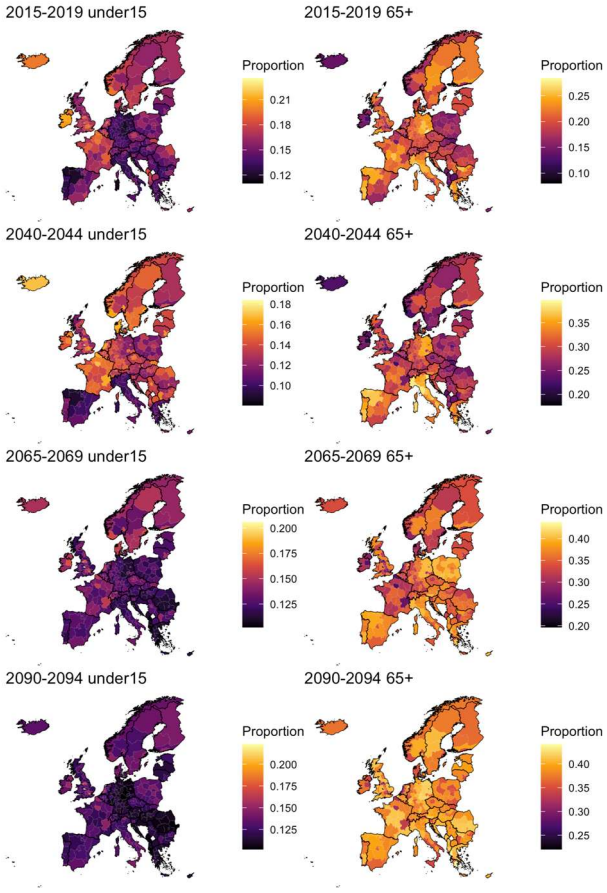

Figure 8: Population projections, age group proportions for the age groups 'Under 15' and '65+' for SSP 2.

Secondly, we validate the results from a geographical perspective (Figure 8). Here we can clearly reaffirm that Europe will experience significant population aging across all its NUTS-2 regions. At the same time, the socio-economic characteristics of different regions play a crucial role in determining both the intensity and pace of this process. Regions that contain or correspond to a country's major urban centers tend to experience a slower increase in population aging. This pattern is particularly evident in countries such as Austria and the Czech Republic, where the capital city is not only the largest urban center—without any comparable counterpart within the country—but also corresponds administratively to an entire NUTS-2 region.

This trend is also highly pronounced in the United Kingdom, Scandinavia, and the regions that formerly constituted the German Democratic Republic. In contrast, Southern European countries, including Italy, Spain, Portugal, and Greece, exhibit extreme levels of population aging.

Italy presents an interesting case, as urbanization levels do not appear to play a significant role in shaping aging patterns in the central and northern regions, in contrast to many other European areas. Additionally, the case of Alto Adige/Südtirol stands out, as this region exhibits higher fertility rates and a slower decline in the 'Under 15' age group compared to the national trend.

Another key feature of our results is their alignment with the SSPs narratives. As shown in Figure 9, the different national-level scenarios influence general development trends and aging intensity at the subnational level. Although it may not be immediately apparent at this finer spatial resolution, subnational SSP

projections—such as those for urbanization percentages—do, in fact, drive the age structure projections. At the same time, national-level age structures exhibit variations depending on the specific SSP considered, and these differences are observable at the subnational level as well. Importantly, it is not just the range differences in the legends that stand out; the distinct gradient distribution in the plots underscores the added value of SSP-coherent projections, highlighting their ability to capture complex, nuanced patterns across scales.

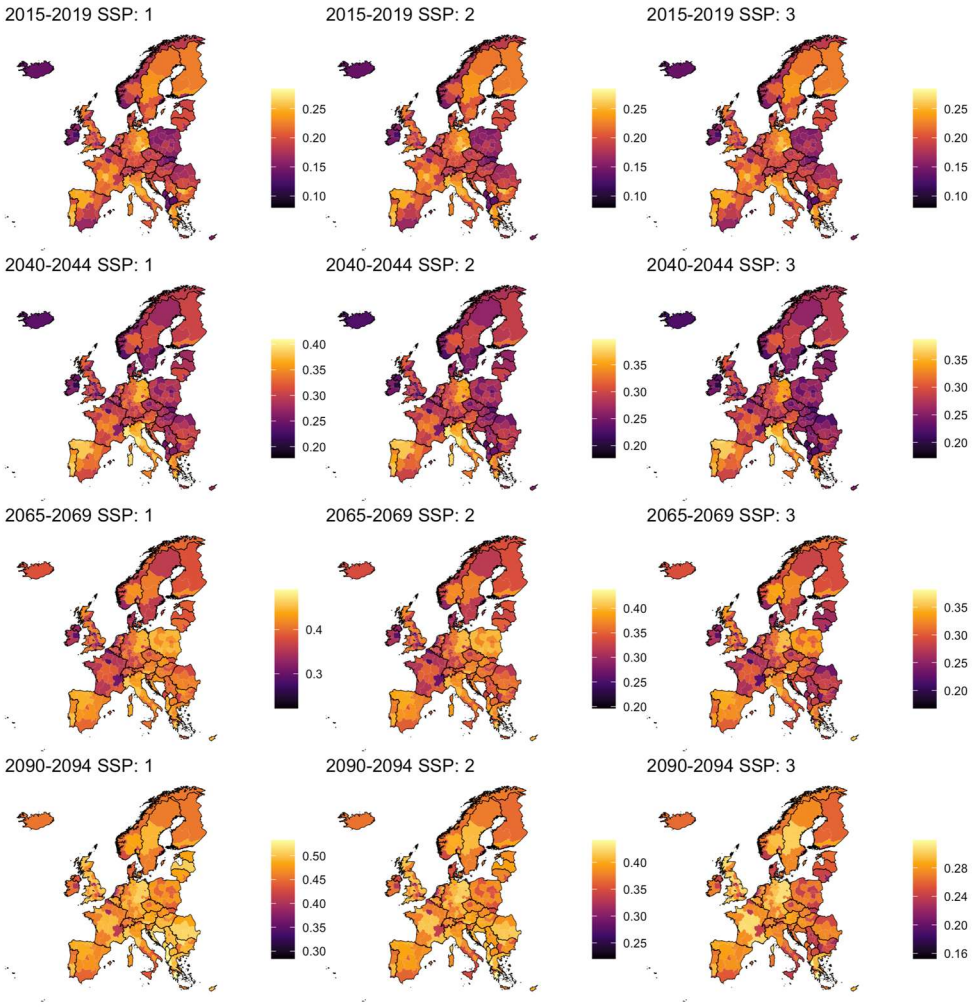

Figure 9: Population projections, age group '65+' according to SSP 1, SSP 2, SSP 3 and period.

4 Discussion and further developments

This study makes two major contributions: (1) a methodological innovation; and (2) projections of future population trajectories until the year 2100, broken down by age at the NUTS-2 level for 34 European countries. The disaggregation is developed in a manner that ensures applicability to different time–space settings. Specifically, we introduced and tested new methodology for geographically disaggregating population projections to the subnational level, using European NUTS-2 regions as our test case. The model is based on an artificial neural network architecture, selected for its flexibility and predictive power. The careful

variables selection process, combined with the application of the Simplified-SIEVE approach, was performed to enhance the interpretability of the results while explicitly accounting for uncertainty. By leveraging this approach, we are able to generate subnational population projections that maintain coherence with the SSPs (Shared Socioeconomic Pathways). The SSPs offer five distinct pathways that reflect varying levels of development, challenges to adaptation, and mitigation, integrating essential factors such as population growth, technological progress, and societal equity. This scenario-based approach allows for a holistic understanding of how different forces interact and provides reliable, consistent projections across multiple models, which is crucial for informing long-term policy decisions.

In addition to the methodological advancement presented, we also add to the existing literature by providing a spatial disaggregation of existing, national-level age structure projections for Europe. The ability to align these projections with the SSPs lends added credibility and robustness to the results, especially considering the long temporal span of the data, which spans 35 years of observed data and includes projections up to the end of the 21st century. However, we also acknowledge that the coherence with SSPs may be both a strength and a limitation. The different publication years and calibration periods for various datasets, as well as the SSPs' focus primarily on national-level projections, leave certain gaps in the subnational dimension, presenting both challenges and opportunities for future research. Additionally, working with administrative boundaries such as the NUTS regions, which have undergone changes over the 35-year period, introduces further complexity in the analysis. Despite these challenges, this work represents an important first step in advancing both the geographical scope and the socioeconomic dimensions of population projections. The regional disparities underlined by our results underscore the need for targeted policy interventions that account for local demographic dynamics. Addressing the challenges posed by population aging requires tailored approaches to service provision, labor market planning, and social welfare policies that reflect the specific needs of different regions. Such interventions would additionally benefit from more precise and informative data; to this end, we aim to refine the methodology by extending the geographical resolution to the NUTS-3 level and incorporating additional socioeconomic dimensions, such as more granular age groups, sex, and educational attainment, while leveraging a broader set of covariates. This potentially adding to the accuracy and relevance of the projections and provide a more nuanced understanding of regional population dynamics in Europe.

References

Basu, Rupa. 2009. 'High Ambient Temperature and Mortality: A Review of Epidemiologic Studies from 2001 to 2008'. *Environmental Health* 8 (1): 40. https://doi.org/10.1186/1476-069X-8-40.

Bosco, Claudio, Natalia Tejedor-Garavito, Daniele de Rigo, et al. 2018. *Geostatistical Tools to Map the Interaction between Development Aid and Indices of Need*. May 1.

Büntgen, Ulf, Willy Tegel, Kurt Nicolussi, et al. 2011. '2500 Years of European Climate Variability and Human Susceptibility'. *Science* 331 (6017): 578–82. https://doi.org/10.1126/science.1197175.

Calleja-Agius, Jean, Kathleen England, and Neville Calleja. 2021. 'The Effect of Global Warming on Mortality'. *Early Human Development* 155 (April): 105222. https://doi.org/10.1016/j.earlhumdev.2020.105222.

Carvalho, Adenilson R., Fernando M. Ramos, and Antonio A. Chaves. 2011. 'Metaheuristics for the Feedforward Artificial Neural Network (ANN) Architecture Optimization Problem'. *Neural Computing and Applications* 20 (8): 1273–84. https://doi.org/10.1007/s00521-010-0504-3.

Chen, Yidan, Fang Guo, Jiachen Wang, Wenjia Cai, Can Wang, and Kaicun Wang. 2020. 'Provincial and Gridded Population Projection for China under Shared Socioeconomic Pathways from 2010 to 2100'. *Scientific Data* 7 (1): 83. https://doi.org/10.1038/s41597-020-0421-y.

Chen, Yimin, Xia Li, Kangning Huang, Ming Luo, and Minyi Gao. 2020. 'High-Resolution Gridded Population Projections for China Under the Shared Socioeconomic Pathways'. *Earth's Future* 8 (6): e2020EF001491. https://doi.org/10.1029/2020EF001491.

De Rigo, D., A. Castelletti, A.E. Rizzoli, R. Soncini-Sessa, and E. Weber. 2005. 'A SELECTIVE IMPROVEMENT TECHNIQUE FOR FASTENING NEURO-DYNAMIC PROGRAMMING IN WATER RESOURCE NETWORK MANAGEMENT'. *IFAC Proceedings Volumes* 38 (1): 7–12. https://doi.org/10.3182/20050703-6-CZ-1902.02172.

Dimitrova, Anna. 2021. 'Seasonal Droughts and the Risk of Childhood Undernutrition in Ethiopia'. *World Development* 141 (May): 105417. https://doi.org/10.1016/j.worlddev.2021.105417.

Engelbrecht, Andries Petrus. 2001. 'Sensitivity Analysis for Selective Learning by Feedforward Neural Networks'. *Fundam. Informaticae* 46: 219–52.

European Environment Agency. 2024. *European Climate Risk Assessment: Executive Summary.* Publications Office. https://data.europa.eu/doi/10.2800/204249.

Eurostat 2024, 2024. n.d. https://ec.europa.eu/eurostat/web/nuts/history.

Freudenreich, Hanna, Anastasia Aladysheva, and Tilman Brück. 2022. 'Weather Shocks across Seasons and Child Health: Evidence from a Panel Study in the Kyrgyz Republic'. *World Development* 155 (July): 105801. https://doi.org/10.1016/j.worlddev.2021.105801.

Gao, Jing. 2017. *Downscaling Global Spatial Population Projections from 1/8-Degree to 1-Km Grid Cells*. With University Corporation For Atmospheric Research (UCAR):National Center For Atmospheric Research (NCAR):NCAR Library (NCARLIB). UCAR/NCAR. Application/pdf, 2082 KB. https://doi.org/10.5065/D60Z721H.

Gao, Jing. 2020. 'Global 1-Km Downscaled Population Grids, SSP-Consistent Projections and Base Year, v1.01 (2000 - 2100)'. Version 1.0. With Jing Gao. Harvard Dataverse. https://doi.org/10.7910/DVN/TLJ99B.

Gao, Jing, and Martino Pesaresi. 2021. 'Downscaling SSP-Consistent Global Spatial Urban Land Projections from 1/8-Degree to 1-Km Resolution 2000–2100'. *Scientific Data* 8 (1): 281. https://doi.org/10.1038/s41597-021-01052-0.

García-León, David, Pierre Masselot, Malcolm N Mistry, et al. 2024. 'Temperature-Related Mortality Burden and Projected Change in 1368 European Regions: A Modelling Study'. *The Lancet Public Health* 9 (9): e644–53. https://doi.org/10.1016/S2468-2667(24)00179-8.

Hauer, Mathew E. 2019. 'Population Projections for U.S. Counties by Age, Sex, and Race Controlled to Shared Socioeconomic Pathway'. *Scientific Data* 6 (1): 190005. https://doi.org/10.1038/sdata.2019.5.

Hornik, Kurt, Maxwell Stinchcombe, and Halbert White. 1990. 'Universal Approximation of an Unknown Mapping and Its Derivatives Using Multilayer Feedforward Networks'. *Neural Networks* 3 (5): 551–60. https://doi.org/10.1016/0893-6080(90)90005-6.

Jesus, Ricardo J., Mário L. Antunes, Rui A. Da Costa, Sergey N. Dorogovtsev, José F. F. Mendes, and Rui L. Aguiar. 2021. 'Effect of Initial Configuration of Weights on Training and Function of Artificial Neural Networks'. *Mathematics* 9 (18): 2246. https://doi.org/10.3390/math9182246.

Jylhä, Kirsti, Heikki Tuomenvirta, Kimmo Ruosteenoja, Hanna Niemi-Hugaerts, Krista Keisu, and Juha A. Karhu. 2010. 'Observed and Projected Future Shifts of Climatic Zones in Europe and Their Use to Visualize Climate Change Information'. *Weather, Climate, and Society* 2 (2): 148–67. https://doi.org/10.1175/2010WCAS1010.1.

Kang, Youngeun, and Gyoungju Lee. 2024. 'Spatiotemporal Population Projections within the Framework of Shared Socioeconomic Pathways: A Seoul, Korea, Case Study'. *Sustainability* 16 (13): 5719. https://doi.org/10.3390/su16135719.

Kashnitsky, Ilya, and Jonas Schöley. 2018. 'Regional Population Structures at a Glance'. *The Lancet* 392 (10143): 209–10. https://doi.org/10.1016/S0140-6736(18)31194-2.

KC, Samir, Moradhvaj, Michaela Potancokova, et al. 2024a. 'Wittgenstein Center (WIC) Population and Human Capital Projections - 2023'. Version V13. Zenodo, February 7. https://doi.org/10.5281/ZENODO.10618931.

KC, Samir, Moradhvaj, Michaela Potancokova, et al. 2024b. 'Wittgenstein Center (WIC) Population and Human Capital Projections - 2023'. Version V13. Zenodo, February 7. https://doi.org/10.5281/ZENODO.7767425.

Lutz, Wolfgang, William P. Butz, and Samir KC. 2014. *World Population and Human Capital in the Twenty-First Century*. Oxford university press.

McCulloch, Warren S., and Walter Pitts. 1943. 'A Logical Calculus of the Ideas Immanent in Nervous Activity'. *The Bulletin of Mathematical Biophysics* 5 (4): 115–33. https://doi.org/10.1007/BF02478259.

McDermott-Levy, Ruth, Madeline Scolio, Kabindra M. Shakya, and Caroline H. Moore. 2021. 'Factors That Influence Climate Change-Related Mortality in the United States: An Integrative Review'. *International Journal of Environmental Research and Public Health* 18 (15): 8220. https://doi.org/10.3390/ijerph18158220.

McMichael, Anthony. 2014. 'Climate Change and Children: Health Risks of Abatement Inaction, Health Gains from Action'. *Children* 1 (2): 99–106. https://doi.org/10.3390/children1020099.

Merkle, M., O. Dellaccio, R. Dunford, et al. 2023. 'Creating Quantitative Scenario Projections for the UK Shared Socioeconomic Pathways'. *Climate Risk Management* 40: 100506. https://doi.org/10.1016/j.crm.2023.100506.

Nguyen, D., and B. Widrow. 1990. 'Improving the Learning Speed of 2-Layer Neural Networks by Choosing Initial Values of the Adaptive Weights'. *1990 IJCNN International Joint Conference on Neural Networks*, 21–26 vol.3. https://doi.org/10.1109/IJCNN.1990.137819.

Nikelshpur, Dmitry, and Charles C. Tappert. 2013. 'Using Particle Swarm Optimization to Pre-Train Artificial Neural Networks: Selecting Initial Training Weights for Feed-Forward Back-Propagation Neural Networks'. https://api.semanticscholar.org/CorpusID:16543869.

Rai, Masna, Susanne Breitner, Kathrin Wolf, Annette Peters, Alexandra Schneider, and Kai Chen. 2022. 'Future Temperature-Related Mortality Considering Physiological and Socioeconomic Adaptation: A Modelling Framework'. *The Lancet Planetary Health* 6 (10): e784–92. https://doi.org/10.1016/S2542-5196(22)00195-4.

Raudys, S., and M. Skurikhina. 1992. 'The Role of the Number of Training Samples on Weight Initialisation of Artificial Neural Net Classifier'. *[Proceedings] 1992 RNNS/IEEE Symposium on Neuroinformatics and Neurocomputers*, 343–53 vol.1. https://doi.org/10.1109/RNNS.1992.268553.

Rosenblatt, F. 1958. 'The Perceptron: A Probabilistic Model for Information Storage and Organization in the Brain.' *Psychological Review* 65 (6): 386–408. https://doi.org/10.1037/h0042519.

Rumelhart, David E., Geoffrey E. Hinton, and Ronald J. Williams. 1986. 'Learning Representations by Back-Propagating Errors'. *Nature* 323 (6088): 533–36. https://doi.org/10.1038/323533a0.

Schmidhuber, Jürgen. 2015. 'Deep Learning in Neural Networks: An Overview'. *Neural Networks* 61 (January): 85–117. https://doi.org/10.1016/j.neunet.2014.09.003.

Son, Ji-Young, Jia Coco Liu, and Michelle L Bell. 2019. 'Temperature-Related Mortality: A Systematic Review and Investigation of Effect Modifiers'. *Environmental Research Letters* 14 (7): 073004. https://doi.org/10.1088/1748-9326/ab1cdb.

Striessnig, Erich, Jing Gao, Brian C O'Neill, and Leiwen Jiang. 2019. 'Empirically Based Spatial Projections of US Population Age Structure Consistent with the Shared Socioeconomic Pathways'. *Environmental Research Letters* 14 (11): 114038. https://doi.org/10.1088/1748-9326/ab4a3a.

Székely, Gábor J., Maria L. Rizzo, and Nail K. Bakirov. 2007. 'Measuring and Testing Dependence by Correlation of Distances'. *The Annals of Statistics* 35 (6). https://doi.org/10.1214/009053607000000505.

Terama, Emma, Elizabeth Clarke, Mark D. A. Rounsevell, Stefan Fronzek, and Timothy R. Carter. 2019. 'Modelling Population Structure in the Context of Urban Land Use Change in Europe'. *Regional Environmental Change* 19 (3): 667–77. https://doi.org/10.1007/s10113-017-1194-5.

Thiede, Brian C., and Clark Gray. 2024. 'Childhood Malnutrition and Mortality in a Changing Climate'. Preprint, August 8. https://doi.org/10.31235/osf.io/e3ksy.

Van Ruijven, Bas J., Marc A. Levy, Arun Agrawal, et al. 2014. 'Enhancing the Relevance of Shared Socioeconomic Pathways for Climate Change Impacts, Adaptation and Vulnerability Research'. *Climatic Change* 122 (3): 481–94. https://doi.org/10.1007/s10584-013-0931-0.

Wang, Xinyu, Xiangfeng Meng, and Ying Long. 2022. 'Projecting 1 Km-Grid Population Distributions from 2020 to 2100 Globally under Shared Socioeconomic Pathways'. *Scientific Data* 9 (1): 563. https://doi.org/10.1038/s41597-022-01675-x.

Ward, Joe H. 1963. 'Hierarchical Grouping to Optimize an Objective Function'. *Journal of the American Statistical Association* 58 (301): 236–44. https://doi.org/10.1080/01621459.1963.10500845.

Weeda, Lewis J.Z., Corey J.A. Bradshaw, Melinda A. Judge, Chitra M. Saraswati, and Peter N. Le Souëf. 2024. 'How Climate Change Degrades Child Health: A Systematic Review and Meta-Analysis'. *Science of The Total Environment* 920 (April): 170944. https://doi.org/10.1016/j.scitotenv.2024.170944.

White, Halbert. 1989. 'Learning in Artificial Neural Networks: A Statistical Perspective'. *Neural Computation* 1 (4): 425–64. https://doi.org/10.1162/neco.1989.1.4.425.

Willmott, Cj, and K Matsuura. 2005. 'Advantages of the Mean Absolute Error (MAE) over the Root Mean Square Error (RMSE) in Assessing Average Model Performance'. *Climate Research* 30: 79–82. https://doi.org/10.3354/cr030079.

Xu, Wenru, Yuyu Zhou, Hannes Taubenböck, et al. 2024. 'Spatially Explicit Downscaling and Projection of Population in Mainland China'. *Science of The Total Environment* 941 (September): 173623. https://doi.org/10.1016/j.scitotenv.2024.173623.

Zou, Jinming, Yi Han, and Sung-Sau So. 2008. 'Overview of Artificial Neural Networks'. In *Artificial Neural Networks*, edited by John M. Walker, vol. 458, edited by David J. Livingstone. Methods in Molecular Biology™. Humana Press. https://doi.org/10.1007/978-1-60327-101-1_2.

Supplementary material

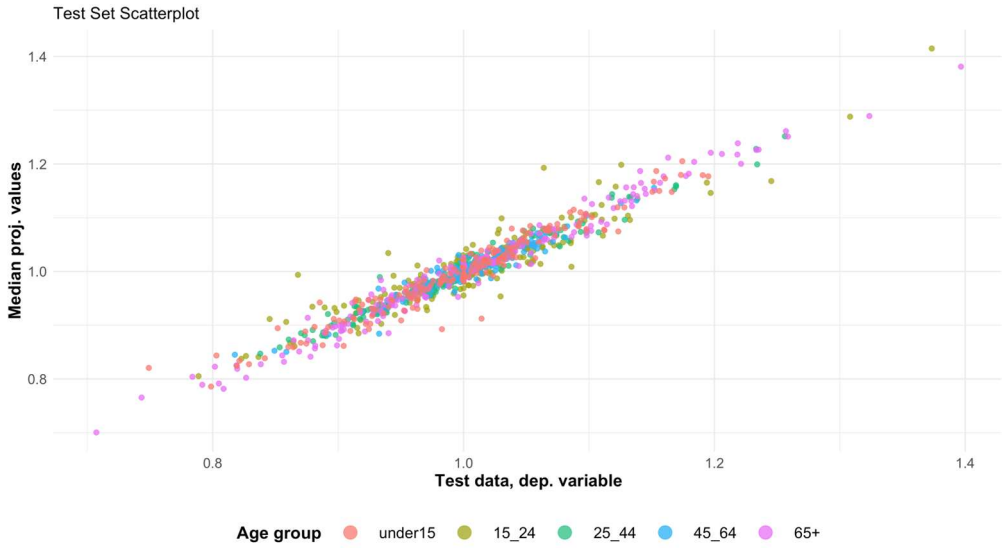

Figure 4: test-set scatterplot

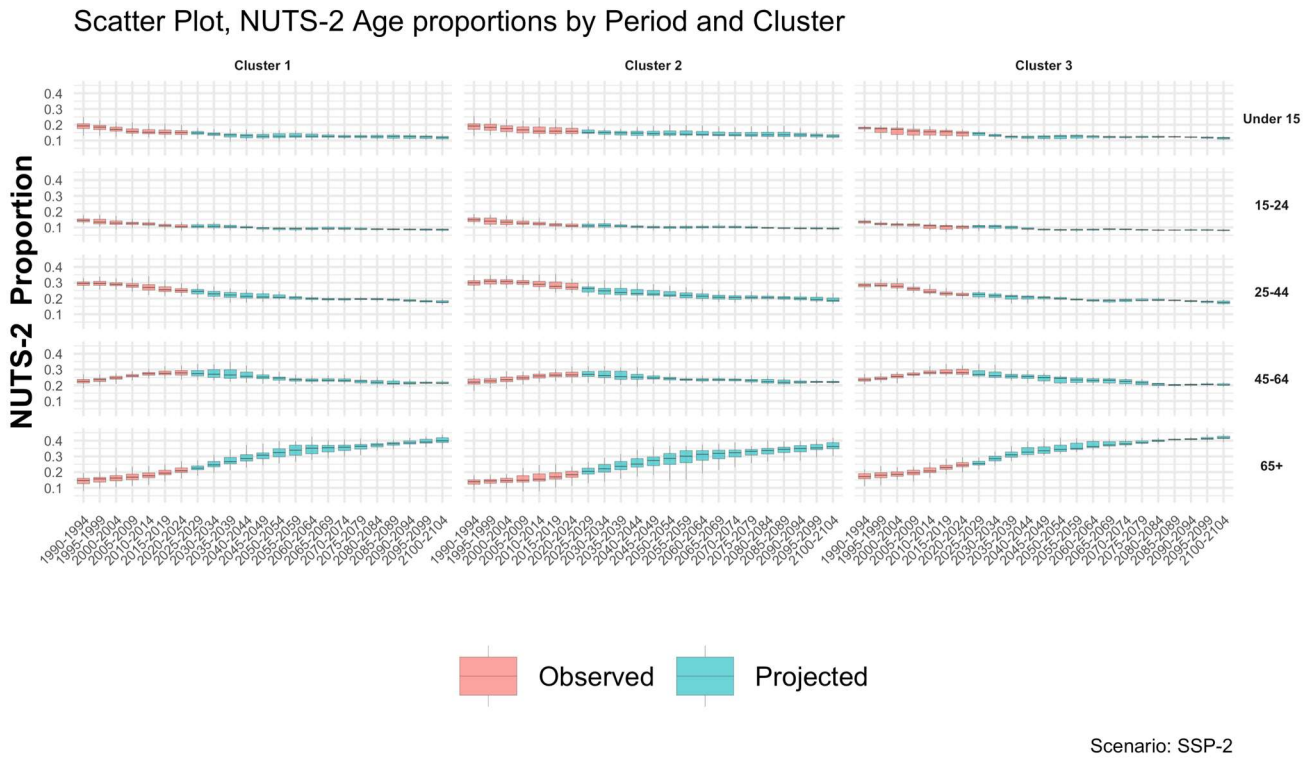

Table A1.1 – Variables list

Variable Code	Variable Meaning
g.pop.NUTS2	Growth of the population in NUTS-2 region
lag1.tot_pop_NUTS2	5-years lag tot. pop. In NUTS-2 region
lag2.tot_pop_NUTS2	10-years lag tot. pop. In NUTS-2 region
lag1ratio.tot_pop_NUTS2	Ratio of 5- and 10-years lag tot. pop. in NUTS-2 region
lag1_under15	5-years lag under 15 pop
lag1_15_24	5-years lag under 15-24 pop
lag1_25_44	5-years lag under 25-44 pop
lag1_45_64	5-years lag under 45-64 pop
lag1_65	5-years lag under 65+ pop
lag2_under15	10-years lag under 15 pop
lag2_15_24	10-years lag 15-24 pop
lag2_25_44	10-years lag 25-44 pop
lag2_45_64	10-years lag 45-64 pop
lag2_65	10-years lag 65+ pop
lag1_g_under15	5-years lag growth under 15 pop
lag1_g_15_24	5-years lag growth 15-24 pop
lag1_g_25_44	5-years lag growth 25-44 pop
lag1_g_45_64	5-years lag growth 45-64 pop
lag1_g_65	5-years lag growth 65+ pop
lag1_quot_under15	Ratio between regional and national proportion, age under 15, 5-years lag.
lag1_quot_15_24	Ratio between regional and national proportion, age 15-24, 5-years lag.
lag1_quot_25_44	Ratio between regional and national proportion, age 25-44, 5-years lag.
lag1_quot_45_64	Ratio between regional and national proportion, age 45-64, 5-years lag.
lag1_quot_65	Ratio between regional and national proportion, age 65+, 5-years lag.
lag2_quot_under15	Ratio between regional and national proportion, age under 15, 10-years lag.
lag2_quot_15_24	Ratio between regional and national proportion, age 15-24, 10-years lag.
lag2_quot_25_44	Ratio between regional and national proportion, age 25-44, 10-years lag.
lag2_quot_45_64	Ratio between regional and national proportion, age 45-64, 10-years lag.
lag2_quot_65	Ratio between regional and national proportion, age 65+, 10-years lag.
ctry_prop_under15	Proportion at the country level
ctry_prop_15_24	Proportion at the country level
ctry_prop_25_44	Proportion at the country level
ctry_prop_45_64	Proportion at the country level
ctry_prop_65	Proportion at the country level
lag1_ctry_prop_under15	Proportion at the country level, 5-years lag
lag1_ctry_prop_15_24	Proportion at the country level, 5-years lag
lag1_ctry_prop_25_44	Proportion at the country level, 5-years lag
lag1_ctry_prop_45_64	Proportion at the country level, 5-years lag
lag1_ctry_prop_65	Proportion at the country level, 5-years lag
lag2_ctry_prop_under15	Proportion at the country level, 10-years lag
lag2_ctry_prop_15_24	Proportion at the country level, 10-years lag
lag2_ctry_prop_25_44	Proportion at the country level, 10-years lag
lag2_ctry_prop_45_64	Proportion at the country level, 10-years lag
lag2_ctry_prop_65	Proportion at the country level, 10-years lag
lag1_ctry_pop_g_under15	Proportional growth of the country population, age under 15, 5 years lag.
lag1_ctry_pop_g_15_24	Proportional growth of the country population, 15-24, 5 years lag.
lag1_ctry_pop_g_25_44	Proportional growth of the country population, 25-44, 5 years lag.
lag1_ctry_pop_g_45_64	Proportional growth of the country population, 45-64 5 years lag.
lag1_ctry_pop_g_65	Proportional growth of the country population, 65+, 5 years lag.
cluster_1	Belongs to cluster 1 (dichotomous variable)
cluster_2	Belongs to cluster 2 (dichotomous variable)
cluster_3	Belongs to cluster 3 (dichotomous variable)
urb_frac	Percentage of urbanised surface in the NUTS-2 region.

	SSP1		SSP2	SSP3	SSP4		SSP5	
Country Grouping								
	HiFert	LoFert			HiFert	LoFert	HiFert	LoFert
Population								
Fertility	Low	Low10	Med	High	High	Low	Low	Low10
Mortality	Low		Med	High	High	Med	Low	
Migration	Med		Med	Low	Med		High	

Note:

• The classification of European countries into 'High-Fertility' and 'Low-Fertility' groups for the purpose of these assumptions can be found in Appendix Table Af1 of the source document.

• For SSP 2, there are additional variants (not shown here for brevity) that consider double and zero net migration.

• The terms 'Low10' and the specific mortality levels (e.g., Med, High) refer to defined scenarios within the WIC projection methodology, the details of which are elaborated in Section 2 of the source document.